Mamoru Iwata*
Mitsumasa Midorikawa
Kazuhisa Koyano

DOI: 10.1002/stco.201810006

# Buckling-restrained brace with high structural performance

*The authors have studied the buckling-restrained brace providing a stable hysteretic characteristic even under high-strain conditions. The structural performance of the buckling-restrained brace is represented by the evaluation formula that is the lower limit of the cumulative plastic strain energy ratio. However, as earthquakes are becoming much longer, so it is necessary to research and develop a new buckling-restrained brace with a higher energy dissipation capacity. In this paper, our past studies are reviewed and the conditions of high-performance of buckling-restrained braces extracted. The buckling-restrained brace considered was tested. As a result, a buckling-restrained brace with a larger cumulative plastic strain energy ratio is proposed.*

## 1 Introduction

A buckling-restrained brace (hereinafter referred to as BRB) has a core plate that transmits axial force and is stiffened by a restraining part to prevent low-order-mode buckling. BRBs deliver equal performance against tensile and compressive forces, and provide stable hysteresis characteristics [1].

Fig. 1 shows the BRB we have been studying. The BRB was prepared by welding together a core plate covered with clearance-adjusting material and a pair of steel mortar planks (mortar-filled steel channels).

We conducted comparative performance tests on the BRB. Specimens having core plates of varying cross-sectional area, width-to-thickness ratio and slenderness ratio, along with those with restraining parts having a varying geometrical moment of inertia, were fabricated for testing purposes. According to [2], structural performance requirements are effectively fulfilled given that the cumulative plastic strain energy ratio $\omega_u$ calculated from the test results (experimental value) exceeds the value obtained from formulae that express the minimum performance value (required value) $\omega_r$.

As illustrated in Fig. 2, the cumulative plastic strain energy ratio $\omega_u$ is a parameter found by dividing the buckling-restrained brace's cumulative plastic strain energy $E_t$, which is calculated from the brace's hysteresis characteristics, by $W_y$, which is obtained by multiplying the core plate's yield load $P_y$ by its elastic-limit deformation $\delta_y$, and then non-dimensionalizing the results of the calculation.

* Corresponding author:
iwata@kanagawa-u.ac.jp

Based on the results of our past studies, this study reviewed in detail the factors that determine the experimental value $\omega_u$. Moreover, based on the review results obtained, we fabricated specimens using the factors that determined the experimental value $\omega_u$ as parameters, and conducted full-scale loading tests to confirm the performance of a BRB with a larger $\omega_u$. Based on the loading test results, we were able to specify the prerequisites for a feasible BRB with a larger $\omega_u$.

## 2 Results obtained from past studies and test model used

### 2.1 Test model

Fig. 3 shows the test model used in past studies. The model represents a building in which BRBs are incorporated. The testing assumes that shear deformation occurs in the building under the influence of horizontal force. In the figure, the core plate length $l_B$ is obtained by subtracting the length

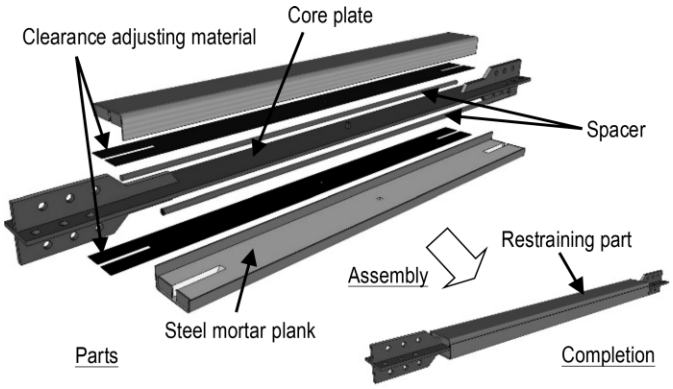


*Fig. 1. Buckling-restrained brace*

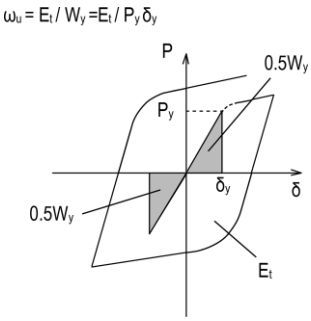


*Fig. 2. Conceptual diagram of $\omega_u$ calculation*

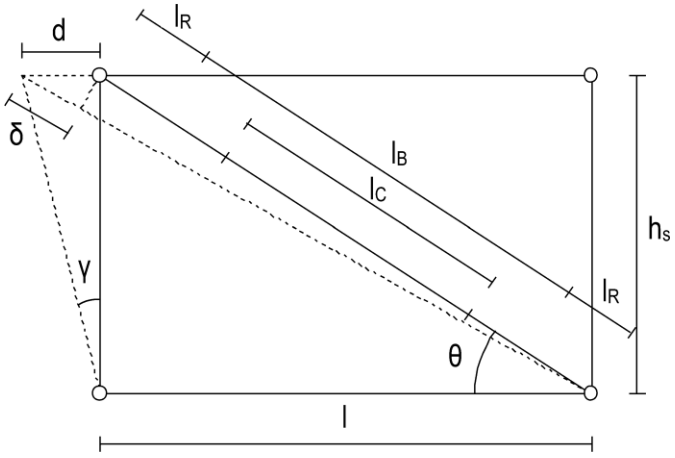


*Fig. 3. Test model*

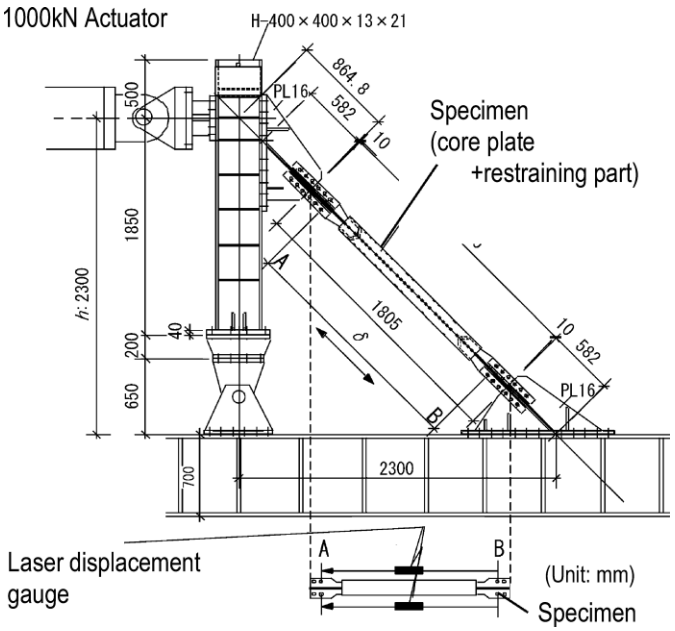


*Fig. 4. An example of loading equipment*

of the rigid zone at both ends $l_R$ from the BRB length. The ratio of core plate length $l_B$ to core plate plastic zone length $l_C$ is defined as the plastic length ratio (= $l_C/l_B$).

In a BRB with a plastic length ratio of 50 %, assuming that axial strain occurring in the core plate elastic zone is minute and hence negligible, the axial strain that occurs in the core plate plastic zone ε (hereinafter referred to as core plate axial strain) is nearly identical to the drift angle. This means that core plate axial strain equivalent in magnitude to a drift angle of 1/200 anticipated during medium earthquakes (level 1) is 0.5 %, and core plate axial strain equivalent in magnitude to a drift angle of 1/100 anticipated during large earthquakes (level 2) is 1.0 %.

### 2.2 Loading plan

An example of the loading equipment is presented in Fig. 4. Using a 1000 kN actuator, tests were conducted by applying increasing loads alternately in the positive and negative directions where the loading is controlled by changing the axial displacement of the core plate. As for the loading equipment, the lower part of the column has a pinned support. The specimens are placed at an inclination of 45°.

Loads equivalent in magnitude to a core plate axial strain of 0.5 % anticipated during medium earthquakes (level 1) are applied twice. Loads equivalent in magnitude to a core plate axial strain of 1 % anticipated during large earthquakes (level 2) are applied five times. Loading is continued with a 3 % axial strain until one of the following occurs: 1) major deformation about either the weak or strong axis, 2) specimen strength is reduced to 80 % of its maximum strength, or 3) a tensile fracture.

### 2.3 Test results

Fig. 5 shows the results of tests conducted in our past studies. The vertical axis of the graph represents $\omega_u$ and the horizontal axis the restraining index R, a value found by dividing the Euler buckling load of the restraining part $P_E$ by the yield load of the core plate $P_y$: $R = P_E/P_y$. Core plate length $l_B$ is assigned to buckling length.

In the test results, the ultimate state of the core plate is categorized as local deformation, strong-axis deformation or tensile fracture. Deformation about the weak axis is defined as local deformation, deformation about the strong axis as strong-axis deformation and fracture of the core plate under tension as tensile fracture.

According to [2], $\omega_u$ obtained from tests in which the core plate experiences tensile fracture or strong-axis deformation at its ultimate state tends to be larger than that obtained from tests in which the core plate ultimate state is local deformation. For this reason, the following equations are used to evaluate the performance of a BRB regarding the lower limit of $\omega_u$ (experimental value) for the specimens in which the core plate ultimate state is local deformation as the required value $\omega_r$ of a BRB:

$$\omega_r = 150 \times R \; (R < 6.0), \; \omega_r = 900 \; (R > 6.0) \qquad (1)$$

## 3 Review of past studies

### 3.1 Ultimate state of core plate

As can be seen in Fig. 5, some specimens have extremely large $\omega_u$ values, while others have a slightly smaller $\omega_u$ value in comparison to that obtained from the performance evaluation formula.

The $\omega_u$ value of all specimens where the core plate experienced tensile fracture in the ultimate state is > 1000. This indicates that in order to increase the $\omega_u$ value of a BRB, it is crucial that the core plate functions properly up to nearly the steel's rupture strength without experiencing local or strong-axis deformation.

### 3.2 Restraining index R

Fig. 5 provides the following information:

1) R < 3: Local deformation is most likely to occur.
2) 3 < R < 6: Some specimens experience tensile fracture or strong-axis deformation. Local deformation is observed in many specimens. The value of $\omega_u$ varies widely in this range.
3) 6 < R: Some specimens experience local or strong-axis deformation in the vicinity of R = 6. Where R is larger,

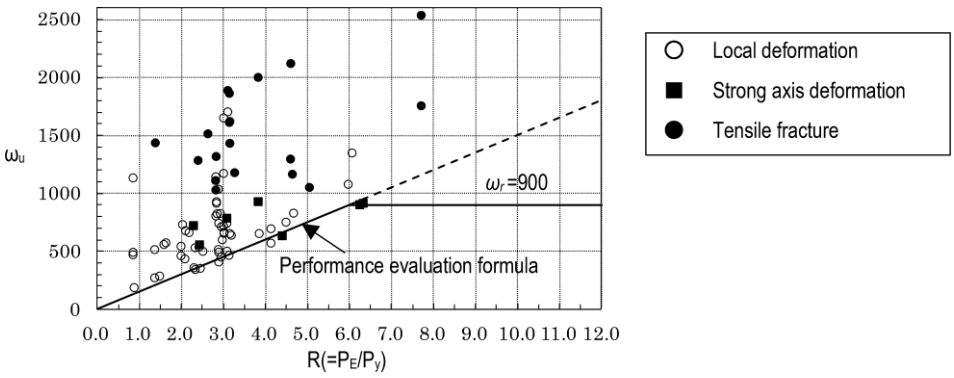


*Fig. 5. $\omega_u$-R relationship*

all specimens experience tensile fracture, along with an increase in the $\omega_u$ value.

### 3.3 Compressive-to-tensile strength ratio α

The compressive-to-tensile strength ratio α is found by dividing the compressive strength $P_c$ by the tensile strength $P_t$, where $P_c$ is the maximum compressive load at each strain amplitude and $P_t$ is the maximum tensile load at each strain amplitude. As α increases, so the specimen's strength on the compression side also increases, leading to potential early-stage local and strong-axis deformation. It was reported in [3] that a high-order buckling mode develops in the core plate plastic zone during compression, and that as the slenderness ratio λ of the core plate plastic zone increases, so the number of points of contact with the restraining part also increases, causing an increase in the frictional force and, ultimately, an increase in α.

### 3.4 Shape and dimension details

1) Area of core plate plastic zone is decreased
   According to [4], many specimens at their ultimate state experienced local deformation in the core plate end sections when the area of the core plate plastic zone was not decreased. To avoid local deformation in the plastic zone end sections, the area of the plastic zone needs to be decreased.
2) Reinforcement around strong axis
   It was stated in [5] that installing a round steel bar on both sides of the core plate is effective in reinforcing the area around the strong axis of the core plate. To further increase $\omega_u$, however, additional reinforcement is necessary. Decreasing the area of the core plate plastic zone and installing a spacer in this narrowed section increases the restraining force about the strong axis.
3) Width-to-thickness ratio
   The ratio of core plate width to core plate thickness is referred to as the width-to-thickness ratio. It was reported in [5] that increasing the width-to-thickness ratio causes early-stage local deformation, resulting in performance degradation. On the other hand, decreasing the width-to-thickness ratio increases strong-axis deformation. In order to reduce local deformation and strong-axis deformation in order to induce tensile fracture, the width-to-thickness ratio should be set at about 6 to 8.
4) Plastic length ratio (= core plate plastic zone length $l_C$/core plate length $l_B$)
   Where the core plate length is the same, λ is increased by increasing the core plate plastic zone length ratio (see [6]). When λ is increased, a high-order buckling mode develops in the core plate plastic zone (see [7]) and frictional force generated by contact with the restraining part increases to increase α. It is appropriate to set the plastic length ratio to 30–50 % in order to suppress an increase in α and induce tensile fracture of the core plate at its ultimate state.
5) Clearance
   It was reported in [5] that the smaller the clearance around the weak axis, the larger is the $\omega_u$ value. However, when the clearance is too small, the restraining part also supports compressive force, causing the α value to increase. According to [5] and [8], a clearance ratio (clearance/core plate thickness) of 10–15 % (sum of clearances on both sides of weak axis) is considered appropriate.
6) Rib penetration length
   Reducing the rib penetration length tends to cause drooping rib ends (see [9]). According to the test results in [6], on BRBs with a small rib penetration length ratio (rib penetration length/core plate plastic zone length) of 9 %, none of BRBs experienced drooping rib ends; however, local deformation occurred. It is considered appropriate to set the rib penetration length ratio to 10–20 %.

## 4 Test Plan

This section describes the performance verification testing of a BRB that meets the conditions for attaining a larger $\omega_u$.

### 4.1 Specimens

Table 1 lists the specimens to be used. Fig. 6 shows a plan view. The core plate is made from steel flats, and strengthening ribs are provided at the ends of the specimens, creating a cruciform cross-section. The core plate is sandwiched between a pair of steel mortar planks that serve as restraining parts. The steel mortar planks are fillet-welded to each other.

The data obtained from core plate and mortar material testing is presented in Table 2. The yield load of the

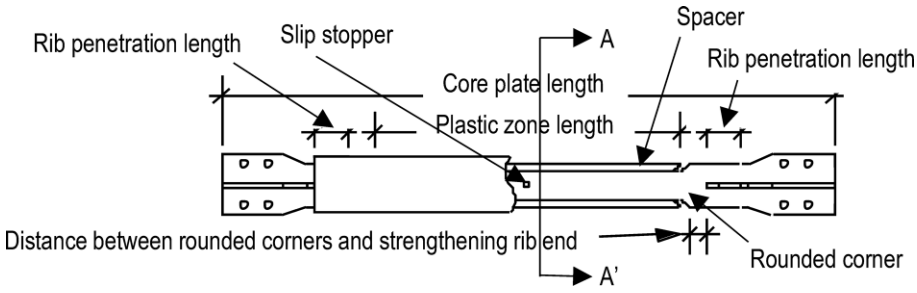


*Fig. 6. Plan view of specimen*

*Table 1. List of specimens*

| Specimens | Core plate | | | | | Restrained part | | |
|---|---|---|---|---|---|---|---|---|
| | Dimensions (mm) | Cross-sectional area ($mm^2$) | $P_y$ (kN) | Core plate length (mm) | Plastic zone length (mm) | h (mm) | b (mm) | $P_E$ (kN) |
| Specimen 1 | PL-84×12 | 1,008 | 308.1 | 1,785 | 892 | 82 | 159.2 | 1,980 |
| Specimen 2 | | | | | 536 | 106 | | 3,427 |
| Specimen 3 | | | 298.3 | | 714 | 82 | | 1,980 |
| Specimen 4 | | | | | 536 | 95 | | 2,701 |
| Specimen 5 | | | 297.5 | | 892 | | | |

*Table 2. Material test results and specimen parameters*

| Specimens | $\sigma_y$ ($N/mm^2$) | Tensile strength ($N/mm^2$) | $\varepsilon_y$ (%) | Compressive strength ($N/mm^2$) | R (=$P_E/P_y$) | Plastic length ratio (%) | Rib penetration length ratio (%) |
|---|---|---|---|---|---|---|---|
| Specimen 1 | 308 | 420 | 0.162 | 72.5 | 6.4 | 50 | 17 |
| Specimen 2 | | | | | 11.0 | 30 | 28 |
| Specimen 3 | 298 | 415 | 0.165 | 64.1 | 6.6 | 40 | 21 |
| Specimen 4 | | | | | 9.0 | 30 | 28 |
| Specimen 5 | | 417 | 0.158 | 71.0 | | 50 | 10 |

core plate $P_y$ is calculated by multiplying the yield stress by the cross-sectional area.

Specimens with varying R, plastic length and rib penetration length ratio are used. These parameters are presented in Table 2.

### 4.2 Loading plan

The test equipment and loading pattern are the same as that used in past studies (see Fig. 4). At maximum axial strain (3%), loading is continued until either the specimen strength drops to 80% of the maximum strength or tensile fracture occurs.

## 5 Test results

### 5.1 Test process and failure mode characteristics

The test process and the failure mode characteristics of the individual specimens are shown in Table 3.

For hysteresis characteristics, the relationship between yield strength ratio β ($P/P_y$; P = axial load) and ε (core plate axial strain (%): ratio of axial deformation to core plate plastic zone length) of specimens 1 and 4 is plotted in Fig. 7.

### 5.2 Failure mode characteristics of core plate

Fig. 8 shows the core plate failure mode characteristics. Specimen 1 experienced local deformation at the strengthening rib end. For the other specimens, local deformation or tensile fracture occurred at the centre of the core plates. Local deformation and tensile fracture locations are indicated with a circle.

## 6 Discussion of test results

### 6.1 Hysteresis characteristics

1) All specimens
   All specimens demonstrated stable spindle-shaped hysteresis characteristics. The yield strength ratio β was found to be approx. 1.5 on the tension side and 1.6–1.7 on the compression side. In all specimens, the yield strength ratio β is larger on the compression side.
2) Specimen 3
   For specimen 3, its strength dropped on the 8th compression with 3% strain; however, loading was continued, since its strength did not drop to 80% of the maximum strength. On the tension side, the specimen's strength did not increase to its maximum strength, and

*Table 3. Testing process and failure mode characteristics and performance evaluation*

| Specimens | Testing process | Failure mode characteristics | $E_t$ (kN/m) | $\omega_u$ |
|---|---|---|---|---|
| Specimen 1 | 5th compression with a 3% strain | Local deformation | 400 | 986 |
| Specimen 2 | 16th tension with a 3% strain | Tensile fracture | 447 | 1,860 |
| Specimen 3 | 9th compression with a 3% strain | Local deformation | 419 | 1,341 |
| Specimen 4 | 18th tension with a 3% strain | Tensile fracture | 507 | 2,162 |
| Specimen 5 | 8th tension with a 3% strain | | 491 | 1,264 |

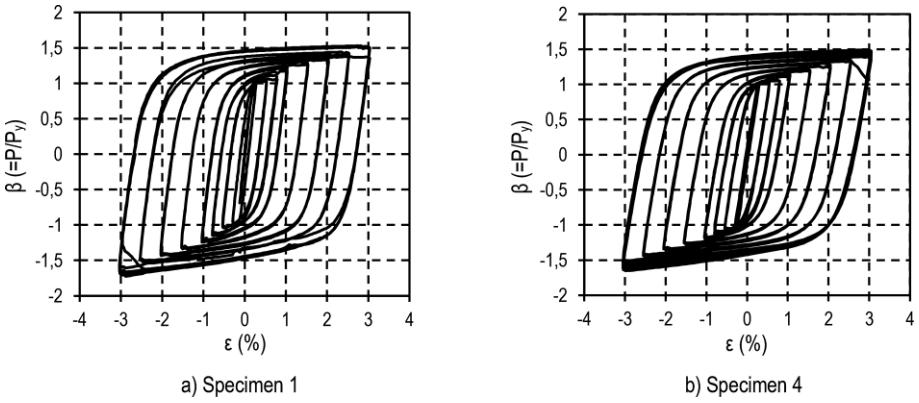


*Fig. 7. β-ε relationship*

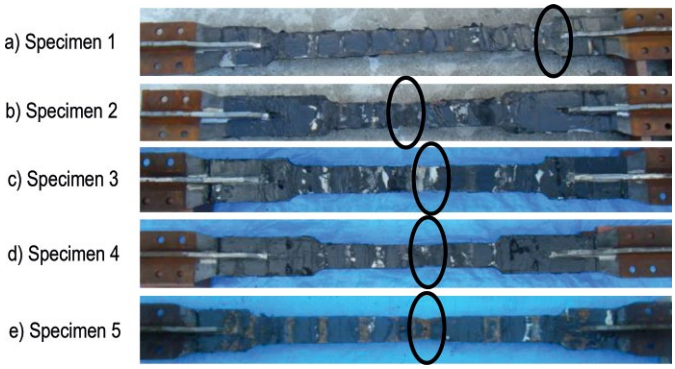


*Fig. 8. Failure mode characteristics of core plate*

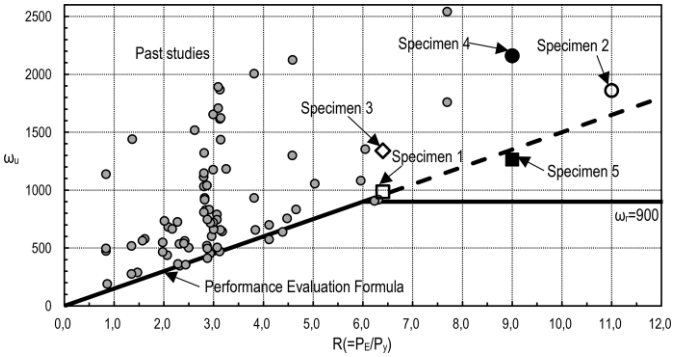


*Fig. 9. $\omega_u$-R relationship*

on the 9th compression with 3% strain, local deformation occurred in the centre of the core plate and its strength dropped to 80% of the maximum strength, whereupon loading was terminated. Local deformation proceeded in this specimen due to its smaller R in comparison to that of the other specimens that experienced tensile fracture.

3) Specimen 5
For specimen 5, although its strength dropped at about 2.5% strain on the 6th tension with 3% strain, loading was continued as the core plate did not fracture. Its strength did not drop under compression. On the 8th tension with 3% strain, tensile fracture occurred in the core plate, whereupon loading was terminated.

### 6.2 Performance evaluation

1) All specimens
Fig. 9 depicts the relationship between $\omega_u$ and R obtained from the results of the test performed in this study and that obtained from past studies. Table 3 shows the values of the cumulative plastic strain energy $E_t$ and $\omega_u$ of the individual specimens. The $\omega_u$ values of all specimens, excluding specimen 1, were > 1200.

2) Specimen 1
For specimen 1, the value of $\omega_u$ is the lowest and local deformation occurred at the rib end. This is attributable to the fact that the location of the narrowed section of the core plate plastic zone with rounded corners coincides with that of the strengthening rib end, causing axial stress to concentrate in the strengthening rib end and induce local deformation.

3) Specimen 3
As in the case of specimen 1, specimen 3 experienced local deformation; however, the location of deformation was found to be the central part of the core plate plastic zone. This suggests that axial stress did not concentrate in the core plate plastic zone end. Given that $\omega_u = 1341$, this specimen ensures adequate performance.

4) Specimen 5
For specimen 5, in which only the distance between the narrowed section of the core plate with rounded

corners and the strengthening rib end is different from that of the other specimens, local deformation did not occur at the end of the core plate plastic zone. This indicates that the distance between the narrowed section of the core plate with rounded corners and the strengthening rib end affects the specimen's performance.

### 6.3 Restraining index R

Specimen 3 experienced local deformation in the central part of the core plate plastic zone at its ultimate state. It is considered that local deformation occurred due to insufficient R. However, $\omega_u$ is large enough; hence, provided that R > 6, this specimen would be capable of delivering adequate performance.

### 6.4 Compressive-to-tensile strength ratio α

1) All specimens
   The graph in Fig. 10 depicts α at the maximum axial strain for the individual specimens. The α values were calculated at each repetition of maximum axial strain (axial strain 3 %).
   All specimens, excluding specimen 3, reached their ultimate state after α exceeded 1.1. For specimens 1 and 5, α is already > 1.1 at the 1st loading, with 3 % strain due to a large plastic length ratio.
2) Specimen 3
   In specimen 3, the value of α drops considerably at the 8th loading. The specimen's strength dropped slightly immediately before the maximum axial strain at the 8th compression; however, loading was continued as its strength did not drop to 80 % of the maximum strength. As a result, its strength did not increase under compression and α remained small.
3) Specimen 5
   For specimen 5, the value of α at the 7th loading with 3 % strain is > 1.15. Its strength dropped immediately before the maximum axial strain at the 7th tension; however, loading was continued as its strength did not drop to 80 % of the maximum strength. As a result, its strength did not increase under tension and α became large.

### 6.5 Influence of core plate end

Only the $\omega_u$ value of specimen 1, which experienced local deformation at the core plate plastic end, is 1200 or less. This indicates that avoiding stress concentration in the core plate plastic zone end is crucial for preventing early-stage strength deterioration.

## 7 Conclusions

Aiming to develop a BRB with a larger cumulative plastic strain energy ratio $\omega_u$, we reviewed the results of our past studies, including fabricated specimens and the verification testing performed. Based on the results of the review and verification testing, this paper presented the prerequisites for a BRB with a larger $\omega_u$.

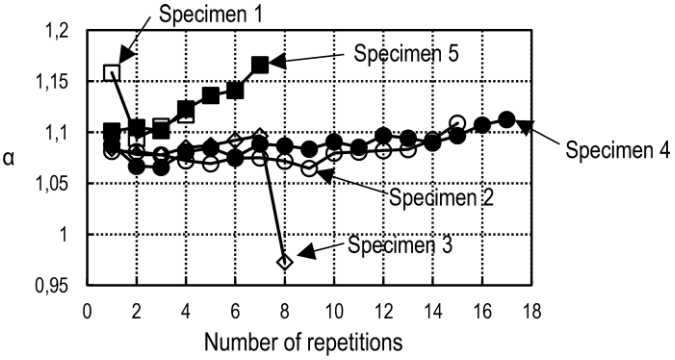


*Fig. 10. Value of α at maximum axial strain*

1. The results of the review of past studies show that in order to attain a larger $\omega_u$, the restraining index R should be set to 6 or higher, the increase in compressive-to-tensile strength ratio α should be limited, the area of the core plate plastic zone should be decreased and a spacer should be installed around the strong axis of the core plate. In addition, the plastic length ratio, width-to-thickness ratio, clearance between core plate and restraining part, rib penetration length and the dimensions of the core plate cross-sectional area are also important considerations.
2. Based on the review results, we fabricated a BRB and performed tests. The test results verify that it is possible to develop a BRB having a larger cumulative plastic strain energy ratio $\omega_u$, as large as > 1200, and a compressive-to-tensile strength ratio α < 1.15.
3. Based on the review and the test results, we presented the prerequisites for a BRB with a larger $\omega_u$. A BRB with a larger $\omega_r$ value can be developed by designing a BRB that meets these prerequisites.

### Acknowledgements

The authors wish to thank Mr. Masatoshi Murai, Chief Engineer at Kanagawa University (at the time this study was performed), Mr. Ryota Iizuka (a graduate student at Kanagawa University (Iwata Laboratory) at the time this study was performed) and members of Iwata Laboratory at Kanagawa University and Midorikawa Laboratory at Hokkaido University for their cooperation during this study.

### References

[1] Iwata, M.; Takeuchi, T.; Fujita, M.: Creation of a Building System. *Japan Steel Structure Journal Co., Ltd.*, Feb 2001.
[2] Iwata, M.; Murai, M.: Buckling-restrained brace using steel mortar planks; performance evaluation as a hysteretic damper. *Earthquake Engineering and Structural Dynamics*, Vol. 35, No. 14, Jul 2006, pp. 1807–1826.
[3] Midorikawa, M.; Tanaka, Y.; Ohtake, M.; Asari, T.; Murai, M.; Iwata, M.: Experimental Study on Buckling-restrained Braces Using Steel Mortar Planks; Evaluation of the Buckling Mode Number and the Relationship between Compression-to-tension Strength ratio and Slenderness Ratio. *Journal of structural and construction engineering, Transactions of AIJ*, Vol. 76, No. 664, Jun 2011, pp. 1153–1160.
[4] Iizuka, R.; Wakayama, T.; Midorikawa, M.; Iwata, M.: Experimental Study on Buckling-restrained Braces Using Steel Mor-

tar Planks; Strong-axis Buckling Mode Due To Difference in Core Plate Slenderness Ratio. *Journal of structural and construction engineering*, *Transactions of AIJ*, Vol. 20, No. 78, Jun 2013, pp. 15–21.

[5] Murase, R.; Murai, M.; Iwata, M.: Experimental Study on Buckling-restrained Braces Using Steel Mortar Planks; Part 4 Effects of core plate width-thickness ratio, restraining force and cross-section details. *Journal of structural and construction engineering*, *Transactions of AIJ*, No. 620, Oct 2007, pp. 117–124.

[6] Tadokoro, A.; Midorikawa, M.; Murai, M.; Iwata, M.: Experimental Study on Buckling-restrained Braces Using Steel Mortar Planks; Influences of Core Plate Length, Plastic Length Ratio and Rib Plate Length. *Journal of structural and construction engineering*, *Transactions of AIJ*, Vol. 74, No. 641, Jul 2009, pp. 1363–1369.

[7] Midorikawa, M.; Wakayama T.; Iizuka, R.; Asari, T.; Murai, M.; Iwata, M.: Experimental Study on Buckling-restrained Braces Using Steel Mortar Planks; Evaluation of the Buckling Mode Number, Compression-to-tension Strength Ratio and Friction Force. *Journal of structural and construction engineering*, *Transactions of AIJ*, Vol. 77, No. 681, Nov 2012, pp. 1763–1771.

[8] Midorikawa, M.; Sasaki, D.; Asari, T.; Murai, M.; Iwata, M.: Experimental Study on Buckling-restrained Braces Using Steel Mortar Planks; Influences of the Clearance Between a Core Plate and a Restraining Member on Compressive Strength and Estimation of the Number of Buckling Modes Related to Compressive Strength. *Journal of structural and construction engineering*, *Transactions of AIJ*, Vol. 75, No. 653, Jul 2010, pp. 1361–1368.

[9] Takeuchi, T.; Matsui, R.; Mihara, S.; Oya, T.; Okamoto, Y.; Ozaki, H.; Iwata, M.: Out-of-plane Mechanical Stability of Buckling-restrained Braces Using Steel Mortar Planks. *AIJ Journal of Technology and Design*, No. 45, Jun 2014, pp. 569–574.

**Keywords:** buckling-restrained brace; structural performance; cumulative plastic strain energy ratio; energy dissipation; compressive-to-tensile strength ratio; hysteresis characteristics; performance evaluation

**Authors**

Professor, Dr.-Eng. Mamoru Iwata
Architecture and Building engineering, Kanagawa University
3-27-1 Rokkakubashi, Kanagawa-ku, Yokohama, 221-8686 Japan
iwata@kanagawa-u.ac.jp

President, Dr.-Eng. Mitsumasa Midorikawa
Professor Emeritus, Hokkaido University
National Research and Development Agency, Building Research Institute
1 Tachihara, Tsukuba, Ibaraki, 305-0802 Japan
midorim@kenken.go.jp

Assistant Professor, Ms.-Eng. Kazuhisa Koyano
Architecture and Building engineering, Kanagawa University
3-27-1 Rokkakubashi, Kanagawa-ku, Yokohama, 221-8686 Japan
koyano@kanagawa-u.ac.jp